OBSERVATION AND MODELIZATION OF THE MECHANISMS OF FRACTURE OF AN AGED DUPLEX STAINLESS STEEL.

P. Joly * and A. Pineau **

Damage mechanisms of an aged duplex stainless steel are presented. Nucleation of cavities in ferrite is strain controlled, and is progressive when plastic deformation increases. Cavities tend to form clusters in a few specific grains. Statistical simulations of the ductility of notched specimens, based on metallographic measurements of the damage, are performed. They represent well the experimental effect of stress triaxiality and of the specimen size on ductility.

INTRODUCTION

It is generally accepted that 3 mechanisms are involved in the fracture of a ductile material. First voids nucleate from hard particles, grow by plastic deformation and coalesce to form a macroscopic crack [1]. So far the analysis of ductile fracture in notched specimens was essentially based on cavity growth, either because voids pre-exist in the material, or because they nucleate at strains small compared to the ductility[2]. In this paper, a model of the damage mechanisms of an aged duplex stainless steel, based on quantitative metallographic observations is presented. It is shown that the nucleation process exceeds the cavity growth and controls the fracture. Furthermore, results of a statistical simulation of ductile fracture in notched specimens illustrate how the experimental scatter and specimen size effect on ductility can be quantitatively related to heterogeneities of the microcracks spatial distribution.

* FRAMATOME Tour Fiat Cedex 16, 92084 PARIS LA DEFENSE.
** Centre des Matériaux, Ecole Nationale Supérieure des Mines de Paris, BP 87, 91003 EVRY Cedex, FRANCE, URA CNRS N°866.

I MATERIAL AND HEAT TREATMENT.

The chemical composition of the investigated CF8M duplex stainless steel is given in Table 1. The alloy contains 20% of ferrite. The material was taken from a centrifugally cast pipe. After a solution treatment at 1115°C and a water quench, the alloy was aged at 400°C for 700 h. During aging, ferrite hardness was increased from 276 to 524 $Hv_{0,05}$. This led to an important embrittlement, as can be seen from the change in Charpy U impact toughness and tensile properties, in Table 2.

Table 1: Chemical composition of the CF8M duplex steel (weight %).

C	Mn	N	Si	Ni	Cr	Mo	Cu	Co	Nb	S	P
0.04	0.76	0.04	1.17	10.03	20.8	2.56	0.15	0.015	0.19	0.001	0.023

Table 2: Mechanical Properties at 20°C before and after aging.

Treatment	Ry MPa	UTS MPa	Elongation %	Reduction of area %	Kcu Toughness daJ/cm^2
Solution	313,5	622	45	66	18
Aged	326	721	21	30	3

II FRACTURE MECHANISMS.

Fracture in the aged alloy also takes place in three steps. First, cleavage cracks are initiated in ferrite. These cleavage cracks cross ferrite and stop at the interface with austenite. They subsequently grow by plastic deformation of austenite. It was shown[3] that the nucleation is controlled by the plastic deformation. This result was consolidated by the evidence that the plastic compatibility stress, depending on the plastic deformation, contributes much more to the local stress in ferrite than the applied macroscopic stress. Local crystallographic orientation has a strong influence on the compatibility stress due to slip modes. Thus only the grains having a favorable orientation will lead to cleavage cracks in ferrite[3]. The microcrack pattern is thus very heterogeneous, as can be seen on Figure 1, with clusters of cracks in these grains[4]. Furthermore, all the cracks do not appear at the same time. The microcrack density increases with plastic deformation[3]. The coalescence, leading to final fracture occurs in one of the clusters of cracks.

III MODELLING.

1- Modelling of the failure of an element of volume.

The most advanced models for ductile failure consider failure as a plastic instability due to the softening effect induced by the porosity. This softening effect can be accounted for, with a yield criterion first introduced by Gurson[5]:

$$\frac{\sigma_{eq}^2}{Y^2} + 2\,q_1\,f\cosh\left(\frac{3\sigma_m}{2Y}\right) - 1 - (q_1 f)^2 = 0 \qquad (1)$$

Y is the flow stress of the matrix and σ_m is the mean stress. It is equivalent to a Mises criterion when f, the volumic fraction of porosity, is zero. Otherwise, the dependence of yielding upon the mean stress, induces a plastic dilation through the normality rule, which represents the cavity growth. In the case of the aged duplex steel, a contribution of strain controlled nucleation, written as follows:

$$df_n = A_n\,d\varepsilon_{eq}^p$$

is added to the part df_g of the increment of porosity due to cavity growth:

$$df = df_g + df_n \qquad (2)$$

Failure is assumed to take place when softening balances strain hardening of the matrix:

$$\frac{d\sigma_{eq}}{d\varepsilon_{eq}^p} = 0 \qquad (3)$$

This condition can be easily numerically computed using equations (1) (2) and the normality rule, neglecting second order terms. General results of this model are presented in ref. (3).

2- Quantitative measurement of material parameters.

The strain hardening curve of the matrix is taken to be the stress-plastic strain curve, measured on a tensile specimen.

Measurements of the cleavage crack area and size were carried out on fractographs of specimens previously prestrained, and heat treated to restore initial ferrite ductility. After fracture, cleavage cracks initiated during the prestrain, appeared clearly on a ductile background[6]. Measurements were then made using image analysis techniques. Assuming that a flat crack is as damaging as a spherical cavity, it can be shown[3] that the equivalent volumic fraction of nucleating cavities f_n is related to the surfacic density of crack Na, through the equation:

$$\frac{df_n}{d\varepsilon_{eq}^p} = \frac{dN_a}{d\varepsilon_{eq}^p} \cdot G$$

where G depends on the area and size of the cracks. It was found that $G = 9.28.10^{-4}$ mm^{-2} . Na was measured on metallographic sections. A procedure based on the Voronoi tesselation (Figure 1), was developped to determine the crack clusters[6]. Thus it was possible to determine the average number of clusters per unit area ($\approx$ 5.7 cm^{-2}), their mean

area ($\approx$ 0.5 mm^2), and their average surfacic nucleation rate $(\frac{dN_a}{d\varepsilon^p_{eq}})$. A sample of 30 clusters was used to determine the distribution of nucleation rates in the cluster population (Figure 2).

3- Simulation of notched axisymmetric specimens.

Experiments were carried out on notched axisymmetric specimens, simulated by finite element (FE), with an elastic plastic code using a Mises yield criterion. The position and the nucleation rate of crack clusters was then randomly generated in the specimens, following the measured data presented above. For each step of loading, in each cluster, the stress triaxiality and the plastic strain, computed by FE was used as input of a postprocessor checking whether the cluster reached the failure criterion (2). Admitting a weakest link hypothesis, when the first cluster fails, the whole specimen breaks.

Two sets of experiments have been simulated: first, ductility results versus stress triaxiality in the center, for specimens with a constant diameter (D=10 mm), and various notch radii (smooth, R=10 mm, 4 mm and 2 mm), are reported in Figure 4. Furthermore, the size effect on ductility was also tested, using specimens with a constant ratio R/D=1.0, and diameters of 6 mm, 10 mm, and 15 mm, as shown on Figure 5.

The effect of stress triaxiality on ductility is correctly reproduced (Figure 4). It has been shown[3] that the strain controlled nucleation accounts for more than 80% of the porosity at fracture, explaining the small effect of hydrostatic stress on ductility, compared to low alloy steels[1]. The effect of specimen size, with a decrease of the average ductility and of the scatter, with increasing diameter, while the minimum ductility remains constant, is correctly reproduced.

CONCLUSIONS.

A model of the mechanisms of fracture of an aged duplex stainless steel was presented. It takes into account the continuous nucleation of cleavage cracks, controlled by plastic strain, and the heterogeneous nature of the crack distribution, through a weakest link theory applied to clusters of cracks. All the parameters of the model are measured independently with metallographic methods. It was shown that:

1- The effect of stress triaxiality on notch ductility is correctly reproduced, thanks to the importance of nucleation with respect to cavity growth.

2- The specimen size effect is also well reproduced. The scatter is thus related to the spatial distribution of weak grains inside the notch and to the distribution of nucleation rate in those grains.

REFERENCES.

(1) A. Pineau and P. Joly, Defect assessment in components, Fundamentals and Applications, J. G. Blauel and K. H. Schwalbe Ed, 1991, pp. 381-414.

(2) F. Mudry, Etude de la Rupture Ductile par clivage d'Aciers Faiblement alliés, PhD Dissertation, Université de Technologie de Compiègne, 1982.

(3) P. Joly, Y. Meyzaud and A. Pineau, Proc. Summer conf. ASME, Scottsdale, Vol. 137, pp. 151-180, 28 April-1 May 1992.

(4) P. Joly, R. Cozar, A. Pineau, Scripta Metallurgica et Materialia, Vol. 24 pp. 2235-2240, 1990.

(5) A. L. Gurson, J. Eng. Mat. Tech. , January 1977, pp. 2-15.

(6) P. Joly, Etude de la Rupture d'Aciers Inoxydables Austeno-Ferritiques Moulés fragilisés par vieillissement à 400°C, PhD dissertation, Ecole des Mines de Paris, to be published 1992.

Acknowledgment: Support from FRAMATOME and the Service Central de Sûreté des Installations Nucléaires is acknowledged.

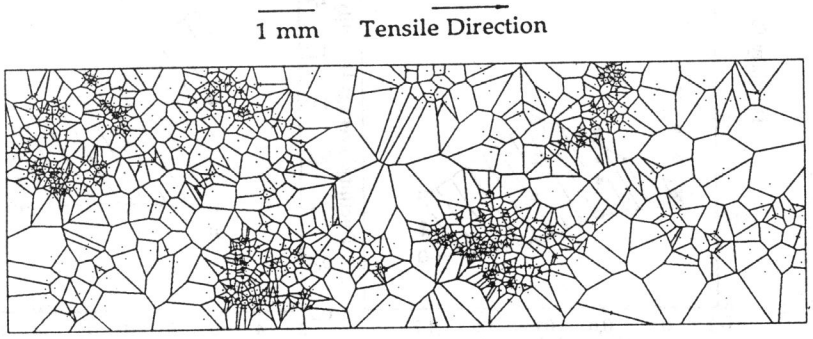

Figure 1: Voronoi tesselation of the cracks (1 point = 1 crack) at εP=16%. Notice the crack clusters.

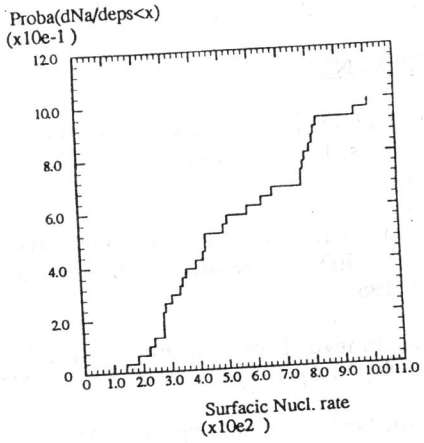

Figure 2: Cumulative probability of nucleation rate in the clusters.

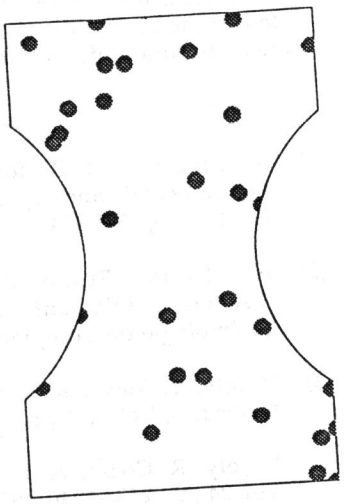

Figure 3: Example of randomly generated clusters in a specimen.

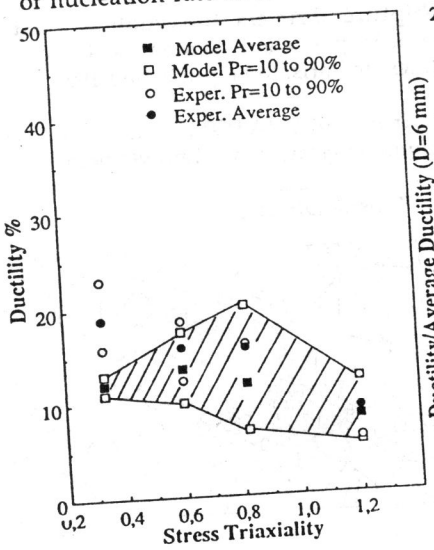

Figure 4: Ductility versus stress triaxiality in notched specimens.

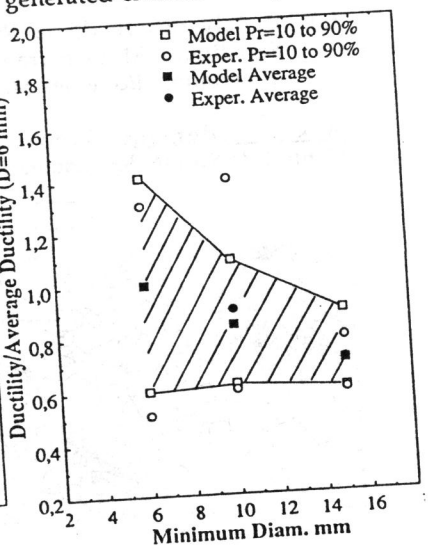

Figure 5: Size effect on the ductility of notched specimens.